Search for diboson resonances with CMS and Pixel Barrel Detector Calibration and Upgrade

Dissertation

zur
Erlangung der naturwissenschaftlichen Doktorwürde
(Dr. sc. nat.)

vorgelegt der Mathematisch-naturwissenschaftlichen Fakultät
der
Universität Zürich

von
Jennifer Ngadiuba

Promotionskomitee

Prof. Dr. Benjamin Kilminster
Prof. Dr. Florencia Canelli
Prof. Dr. Laura Baudis
Prof. Dr. Ueli Straumann

Zürich 2016

Contents

Chapter 1

Introduction

Chapter 2

The Standard Model and beyond

2.1 The Standard Model

2.1.1 Particles and interactions

2.1.2 Spontaneous symmetry breaking

2.1.3 The Higgs mechanism

2.1.4 The Higgs boson discovery at LHC

2.2 The hierarchy problem and other SM limitations

2.3 Theories of new physics

2.3.1 Warped Extra dimensions

2.3.2 Compositeness

2.3.3 Heavy vector triplet

Chapter 3

The CMS Experiment at the LHC

3.1 The Large Hadron Collider

The Large Hadron Collider (LHC) [1] is a proton-proton (pp) collider located at the European Particle Physics Laboratory (CERN) near Geneva, Switzerland. It is situated in the former CERN Large Electron-Positron Collider (LEP) tunnel with a circumference of 27 km about 100 m under ground crossing the border between France and Switzerland. A hadron collider has been chosen to allow higher centre of mass energies compared to electron-positron (e^-e^+) colliders, the latter limited by synchrotron radiation due to the low mass of the particles to be accelerated. High centre of mass energies are required for the production of heavy SM particles such as the top quark and the Higgs boson, and to search for new BSM interactions at the TeV scale. For this purpose, the LHC is designed to produce pp collisions up to a centre of mass energy ($\sqrt{s} = 2E_{beam}$) of 14 TeV, superseding previous high energy hadron colliders by a factor of 7. In addition to colliding protons, the LHC is also capable of accelerating and colliding heavy nuclei, which is, however, not considered in this work.

The LHC is the final element in a succession of machines that accelerate protons to increasingly higher energies. Each machine boosts the energy of a beam of protons, before injecting the beam into the next machine in the sequence. Protons, obtained from a hydrogen source, are first accelerated by a linear accelerator (LINAC 2) to energies of 50 MeV. The beam is then injected into the Proton Synchrotron Booster (PSB), which accelerates the protons to 1.4 GeV, followed by the Proton Synchrotron (PS), which pushes the beam to 25 GeV. Protons are then sent to the Super Proton Synchrotron (SPS) where they are accelerated to 450 GeV. Finally, the beam is injected in the LHC ring, where it completes several revolutions to reach the targeted energy. The LHC ring and the acceleration chain are sketched in Fig. 3.1. Inside the ring, the two proton beams circulate in opposite directions in two tubes kept at ultrahigh vacuum, referred as beam pipes. The acceleration of protons inside LHC is made by radio-frequency cavities (400 MHz), giving a 492 keV energy gain per revolution, with a 7 keV loss per turn due to synchrotron radiation. It takes 4 minutes and 20 seconds to fill each LHC ring, and 20 minutes for the protons to reach their maximum energy of 7 TeV. The maximum energy of the protons is limited by the strength of the magnetic field required for keeping the protons inside the ring. For 7 TeV-protons a magnetic field of 8.3 T has to be produced, which can only be reasonably obtained by superconducting magnets. The ring is equipped with 1232 dipole magnets for bending and 392 quadrupole magnets for focussing made of niobium-titanium (NbTi) are therefore cooled down to a temperature of 1.9 K with the help of super-fluid helium. After acceleration the protons move through the ring in separate bunches of protons with a fixed spatial separation. The LHC ring has four interaction points at which the two counter rotating beams are made to cross and the particle detectors are located. Just prior to collosion, particles from the incoming beams must be squeezed closer together in order to maximize the chances of interaction. For this purpose, a system of three quadrupole magnets, so-called inner triplet, is located at each side of each detector, which squeeze the beams and lead them to collisions in the centre of the detector. Inner triplets tighten the beam, making it 12.5 times narrower from 0.2 mm down to 16 μm across.

Besides the high centre of mass energy required for the production of heavy particles, a high event rate has to be obtained to allow the discovery of processes with low production cross sections. The instantaneous luminosity $\mathcal{L}$ characterizes the interaction rate. For a process with a cross section σ, the interaction rate is given by

$$\frac{dN_{ev}}{dt} = \sigma\mathcal{L}. \tag{3.1}$$

The instantaneous luminosity depends only on the beam parameters and can be written for a Gaussian beam distribution as:

$$\mathcal{L} = \frac{N_b^2 n_b f_{\text{rev}} \gamma_r}{4\pi\sigma_x\sigma_y} \ , \tag{3.2}$$

where N_b is the number of particles per bunch, n_b the number of bunches per beam, f_{rev} the revolution frequency, γ_r the relativistic gamma factor, while σ_x and σ_y characterise the widths of the transverse beam profiles in the horizontal and vertical direction, respectively. The number of interaction events in a period of running time of the collider can be derived as

$$N_{ev} = \sigma \int \mathcal{L}dt = \sigma L \ , \tag{3.3}$$

where L is called the integrated luminosity. It is a measurement of the collected data size and it is usually expressed in inverse of cross section.
The LHC beams can reach very high luminosity with a high frequency bunch crossing and a high density of protons per bunch. In the ring, 2808 bunches of $1.15{\cdot}10^{11}$ protons are circulated, with an average length of 7.5 cm, a width of about 16 μm and a bunch spacing of 25 ns (collision frequency of 40 MHz). This corresponds to the design luminosity of $10^{34}\text{cm}^2\text{s}^1$, which superseds by a factor of 100 the luminosity reached by previous hadron colliders.

Proton collisions take place in four points of the LHC tunnel where the four main experiments are located: ATLAS (*A Toroidal LHC ApparatuS*) [2], CMS (*Compact Muon Solenoid*) [3], LHCb (*LHC beauty experiment*) [4] and ALICE (*A Lead Ion Collider Experiment*) [5]. ATLAS and CMS are general purpose experiments, designed to get an extensive study of SM and BSM physics and to operate at a peak of instantaneous luminosity of $10^{34}\text{cm}^2\text{s}^1$ for pp collisions. The LHCb experiment is instead optimized for bottom quark physics studies while the ALICE experiment is dedicated to the study of the lead-lead collisions with a peak luminosity of $10^{27}\text{cm}^2\text{s}^1$.

LHC operation officially started at the beginning of September 2008 but it was interrupted after a short period, due to the breakdown of superconducting magnets. The collider has been reactivated in November 2009 with first pp collisions at $\sqrt{s} = 900$ GeV, officially starting a new era in the particle physics experiments. Figure 3.2 shows the LHC timeline together with the phases of its operation. The operating center-of-mass energies in pp collisions have so far been 7 TeV in 2010-2011, 8 TeV in 2012 and 13 TeV in 2015-2016. The 7 and 8 TeV periods together make out the *LHC Run 1*, while the 13 TeV period is called the *LHC Run 2*. The work presented in this document is based on both data collected at 8 TeV in 2012 and at 13 TeV in 2015. In the whole Run 1, the LHC operated with a 50 ns bunch spacing. The peak of instantaneous luminosity in 2011 has been $\sim 0.4{\cdot}10^{34}\text{cm}^2\text{s}^1$ for a total delivered integrated luminosity of 6.10 fb^{-1}. In 2012 the beam energy increased to 4 TeV per beam with a peak of instantaneous luminosity of $\sim 0.8{\cdot}10^{34}\text{cm}^2\text{s}^1$ and 23.3 fb^{-1} delivered integrated luminosity by the end of that year. The increment of the instantaneous luminosity leads to a no more negligible number of simultaneous interactions per bunch crossing, the so-called pile-up

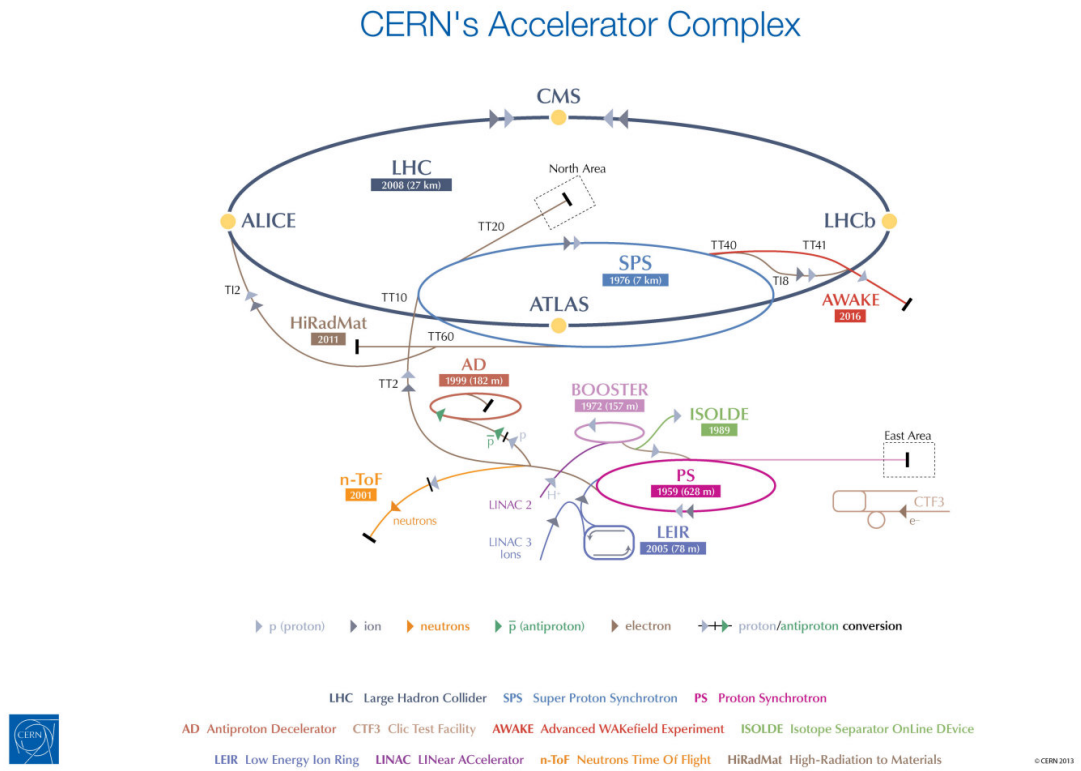

Figure 3.1: The LHC scheme together with its injection chain and the locations of the four main experiments ATLAS, CMS, LHCb and ALICE [6].

(PU) events. It depends on the cross section of inelastic collisions (75 mb at $\sqrt{s} = 7$ TeV- add cite), and it is directly linked to the instantaneous luminosity. The average PU of the data collected in 2012 is equal to 21 (Fig. blabla) while it has been around 15 in 2011 - add cite.

A shut-down period for the LHC (LS1) occurred in the whole 2013 and 2014, where upgrades and technical improvements have been performed in order to reach the designed instantaneous luminosity and centre of mass energy. On March, 21st 2015 the first pp collisions at $\sqrt{s} = 13$ TeV has been obtained, a new record-breaking energy. For the first three months the machine operated with 50 ns bunch spacing while, from August 2015, it has been reduced to the designed 25 ns and the number of bunches per beam has been increased. The first part of this Run 2 phase ended on November 2015 with a total delivered integrated luminosity of 4.22 fb^{-}1 and a peak of instantaneous luminosity of $\sim 0.5 \cdot 10^{34} \mathrm{cm}^2\mathrm{s}^1$ with an average pileup of 12 - add cite. The LHC Run 2 has been restarted in April 2016, after an end-of-the-year technical stop, reaching a peak luminosity of $\sim 1.2 \cdot 10^{34} \mathrm{cm}^2\mathrm{s}^1$ (change this number at some point). The machine has remained in operation at $\sqrt{s} = 13$ TeV for the whole year with a total delivered integrated luminosity of 30 fb^{-1} (change this number at some point). Accordingly to the current LHC schedule, the Run 2 will proceed up to the end of 2018 with a total expected integrated luminosity of 100 fb^{-1}. The data collected in 2016 are not considered in this work.

add some comments about HL-LHC

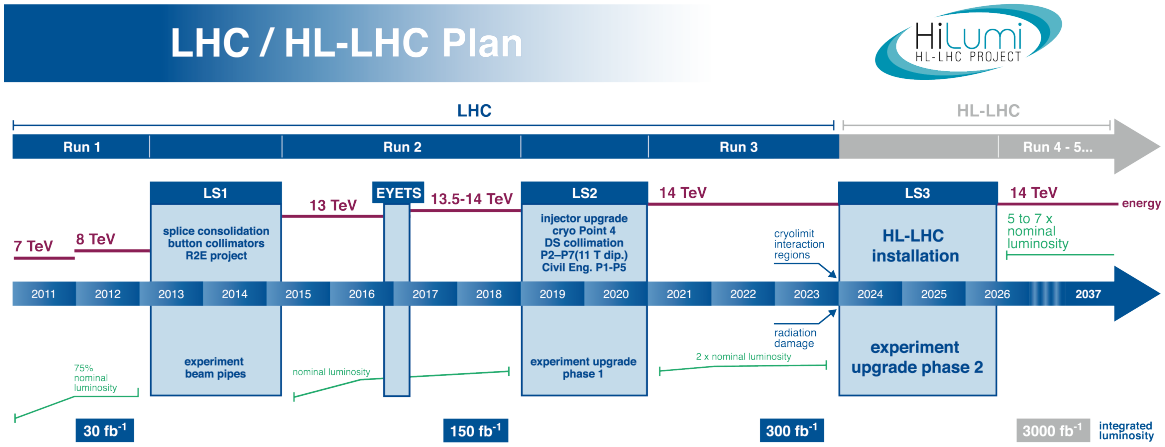

Figure 3.2: LHC timeline.

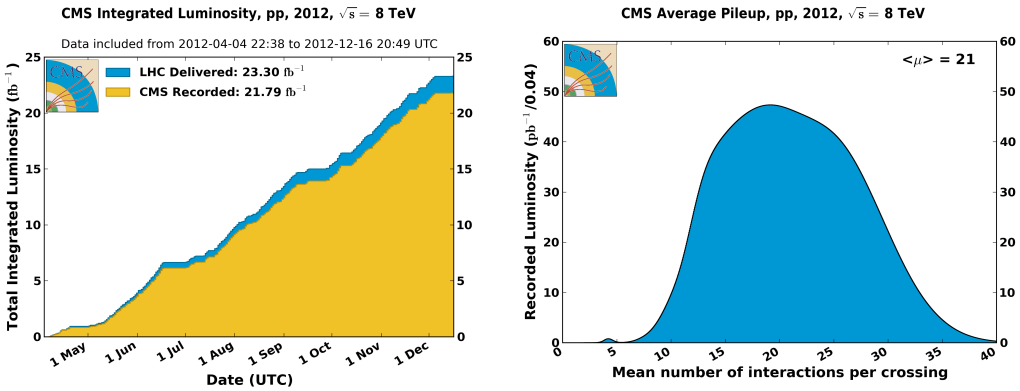

Figure 3.3: Integrated lumi and PU for 2012.

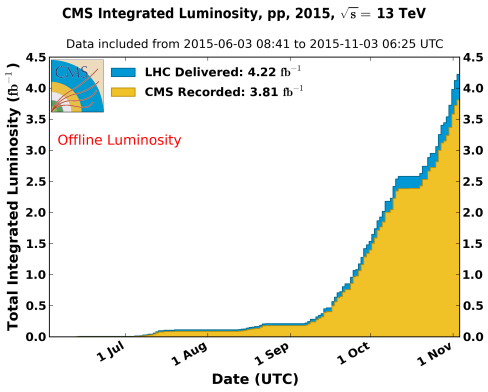

Figure 3.4: Integrated lumi and PU for 2015.

3.2 The CMS Detector

3.2.1 The Silicon Tracker

3.2.2 The Electromagnetic Calorimeter

3.2.3 The Hadronic Calorimeter

3.2.4 The Muon System

3.2.5 The Trigger System

3.3 The CMS detector simulation

Part I

Search for diboson resonances with CMS

Chapter 4

Diboson resonances as signature for new physics

Chapter 5

Event simulation

5.1 Monte Carlo event generators

5.2 Simulation of physics processes

5.2.1 Simulation of signal processes

5.2.2 Simulation of background processes

Chapter 6

Object and event reconstruction

Chapter 7

Boosted H→$b\bar{b}$ and W/Z→$q\bar{q}^{(\prime)}$ identification with jet substructure

---

Chapter 8

Final event selection and categorization

8.1 Search for a WH resonance in the $\ell\nu b\bar{b}$ final state at $\sqrt{s}$ = 8 TeV

8.1.1 $t\bar{t}$ background rejection

8.1.2 Final selection and control plots

8.2 Search for WW/WZ resonances in the $\ell\nu q\bar{q}^{(\prime)}$ final state at $\sqrt{s}$ = 13 TeV

8.2.1 W/Z-jet mass categories

8.2.2 Final selection and control plots

Chapter 9

Background modeling

9.1 W+jets background estimate with alpha method

9.1.1 Description

9.1.2 Extraction of the W+jets normalization

9.1.3 Extraction of the W+jets shape

9.2 Top quark production

9.3 Systematic uncertainties in the background estimation

Chapter 10

Signal modeling and statistical treatment

Chapter 11

Results with 8 TeV data

11.1 Final m_{WH} distribution

11.2 Studies on the excess

11.3 Significance of the data

11.4 Cross section limits

Chapter 12

Results with 13 TeV data

12.1 Final m_{WV} distribution

12.2 Cross section limits

Chapter 13

Combination of searches for diboson resonances at $\sqrt{s} = 8$ and 13 TeV

13.1 Inputs to the combination

13.1.1 8 TeV VV searches

13.1.2 13 TeV VV searches

13.1.3 8 TeV VH searches

13.1.4 13 TeV VH searches

13.2 Combination procedure

13.3 Results

13.3.1 Limits on W'

13.3.2 Limits on Z'

13.3.3 Limits on heavy vector triplet (W'+Z')

13.3.4 Limits on Bulk Graviton

13.3.5 Significance at 2 TeV

Chapter 14

Conclusions

Part II

Calibration and Upgrade of the CMS Pixel Barrel Detector

Chapter 15

introduction chapter: why pixels are so important for physics

Chapter 16

The CMS Pixel Barrel Detector

Chapter 17

Optimization and commissioning for LHC Run II

17.1 Radiation damage after LHC Run I

17.2 Optimization for LHC Run II

17.2.1 Overview of pixel calibrations

17.2.2 Temperature dependence

17.3 Commissioning for LHC Run II

17.3.1 Installation into CMS

17.3.2 Check out of optical connections

17.3.3 Adjustment of readout chain settings

17.3.4 Optimisation of signal performance

Chapter 18

Phase I Upgrade of the CMS Pixel Barrel Detector

Chapter 19

Conclusions

Part III

Summary

Bibliography

[1] L. Evans and P. Bryant, "LHC Machine", *JINST* **3** (2008) S08001.

[2] ATLAS Collaboration, "The ATLAS Experiment at the CERN Large Hadron Collider", *JINST* **3** (2008) S08003, doi:10.1088/1748-0221/3/08/S08003.

[3] CMS Collaboration, "The CMS experiment at the CERN LHC", *JINST* **3** (2008) S08004, doi:10.1088/1748-0221/3/08/S08004.

[4] LHCb Collaboration, "The LHCb Detector at the LHC", *JINST* **3** (2008) S08005, doi:10.1088/1748-0221/3/08/S08005.

[5] ALICE Collaboration, "The ALICE experiment at the CERN LHC", *JINST* **3** (2008) S08002, doi:10.1088/1748-0221/3/08/S08002.

[6] F. Marcastel, "CERN's Accelerator Complex. La chane des acclrateurs du CERN",. General Photo.